Fatigue Performance of Cost Effective Cr-Ni prealloyed PM Steel, designed to replace Fe-Ni Steels and match wrought steels

Alexander Klekovkin, Nagarjuna Nandivada, Ian Howe
North American Höganäs, USA
Sven Bengtsson
Höganäs AB, Sweden

ABSTRACT

Powder Metal materials that exhibit excellent heat treated properties and achieve good fatigue performance are needed to convert wrought components & gears to the PM process as well as to offer a cost effective alternate to existing the FN-020X PM material systems.

North American Höganäs successfully demonstrated the excellent heat treated properties of the new developed prealloyed Cr-Ni steel (Astaloy® CMN). The purpose of this paper is to demonstrate the dynamic properties achievable with this material compared to wrought steels and FN-020X system.

INTRODUCTION

In order to facilitate the penetration of sintered components further into key markets & applications, converting wrought applications to sintered PM, optimized alloy systems are required offering sufficient mechanical performance at an acceptable cost level. Traditionally sintered components have used alloys containing relatively high levels of copper, nickel and molybdenum due to their robustness in manufacturing, particularly sintering due to their low affinity for oxygen.

However, the last three years or so have seen unprecedented volatility in the metal markets leading to very high prices of these traditional alloying elements. This has driven demand by original equipment manufacturers in the automotive value chain for leaner more cost effective materials. The economic recession prevailing at the end of 2008 resulted in a significant drop in metals market prices and apparently the problem dissipated. However, the issue of volatility is not gone as metals prices are expected to rise again during 2009 and 2010 as the global economy emerges from recession into growth, driving demand and prices for metals upwards. Therefore there is a continued need for cost effective PM materials for sintered components.

The Fe – 0.5Cr – 0.5Ni alloy (Astaloy CMN) is intended for highly loaded / stressed applications / components in the heat treated condition[1]. This material provides a chemistry with optimized cost – performance characteristics in the heat treated condition. The combination of low levels of chromium and nickel provides a cost effective alloy, but with sufficient alloy content to provide very good hardenability to produce the desired martensitic microstructure with the hardness and dynamic properties required. Currently, the mainstream PM alloy system used for such applications mentioned above is MPIF FN-020X-HT series[2], containing iron and 2% nickel, and also with copper additions.

This paper sets forth the mechanical properties in heat treated condition, obtainable with the cost effective Fe – 0.5Cr – 0.5Ni alloy (Astaloy CMN) alloy system. In particular dynamic properties will be presented and discussed.

EXPERIMENTAL PROCEDURE

Powders and Materials

The material systems used in the experiments are based on the pre-alloyed Cr-Mo-Ni-Mn steel powder – Astaloy CMN developed in 2008. This is an iron base material prealloyed with Cr, Ni and small amounts of Mo and Mn. Below is shown the chemical composition (Table I), the phase diagram for the nominal composition (Figure 1) and general compressibility curves (Figure 2).

Table I. Chemical composition of Astaloy CMN

Elements	Ni	Cr	Mo	Mn
Wt. %	0.50	0.50	0.10	0.20

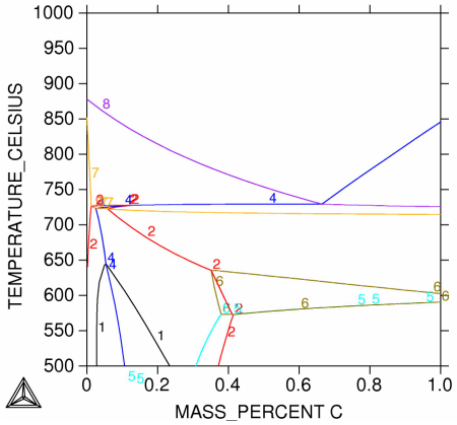

Figure 1. Astaloy CMN phase diagram.

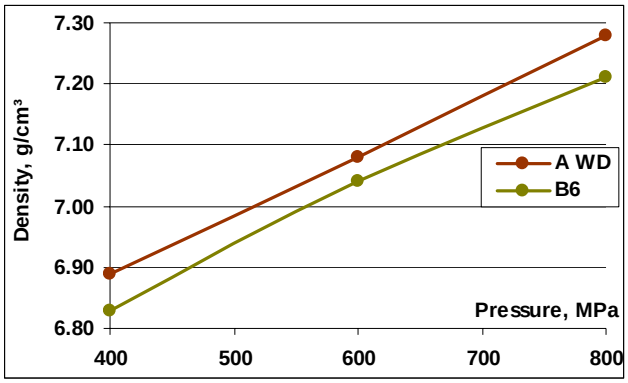

Figure 2. Compressibility curves of Astaloy CMN: AWD– heated die, B6 – RT compaction;

Premixes based on this base powder with the compositions listed in Table II were prepared. Asbury 1651 graphite was used in all cases. The eutectoid point for the alloy is around 0.66%, therefore graphite levels were chosen accordingly. The lubricant used was 0.60% Kenolube from Höganäs AB.

Table II. Materials compositions

Designation	Base Powder	Graphite, %
A	Astaloy CMN	0.25
B6	Astaloy CMN	0.60
B7	Astaloy CMN	0.70*

* for Jominy hardenability and Mass-effect tests.

Sample preparation

Transverse Rupture Strength (TRS), Charpy impact energy (IE) and plane bending Fatigue Strength (FS) bars were compacted from each mix. Material A was compacted to 7.00, 7.20 and 7.30 g/cm³; material B6 – to 7.10 and 7.30; and material B7 – to 7.00 and 7.30 g/cm³. Conventional compaction was used in order to obtain green densities of 7.00, 7.10 and 7.20 g/cm³. To achieve 7.30 g/cm³ the double press – double sinter technique was used: 1st press – 7.10 g/cm³ (593 MPa (43 tsi)); 1st sinter – 787°C (1420°F) for 15 minutes; 2nd press – 7.30 g/cm³ (662 MPa (48 tsi)); 2nd sinter – 1121°C (2050°F).

In addition to test bars, rectangular blocks were compacted from material B7 to green density of 6.90 g/cm³. Jominy hardenability test bars were machined from the blocks according to ASTM standard A255-07. A mass effect study was conducted on cylinders of size Ø25x25 mm and Ø38x38 compacted from material B7 to 7.00 and 7.30 g/cm³. For the case carburization study additional TRS bars were compacted. For a case study FZG gears (OD = 82.26 mm, ID = 30 mm, 16 teeth) were compacted from material A.

Sintering

The test specimens were sintered in conventional nitrogen-hydrogen atmosphere with normal cooling rates (Table III).

Table III. Sintering conditions

Description	N_2/H_2 (N)
Furnace type	Mesh belt
Temperature	1120 °C (2050 °F)
Atmosphere	90%N_2 / 10%H_2
Time at temperature	30 min
Cooling rate	0.5 °C/s (1.0 °F/s)

Heat Treatment

Heat treatment was performed at Pennsylvania Industrial Heat Treaters (St. Mary's, Pennsylvania) based on parameters described in Table IV.

Table IV. Heat treating parameters

Parameters	Material A Case hardening	Material B6 Through hardening	Material B7 Through hardening
Type	Batch	Batch	Batch
Temperature	926 °C (1700 °F)	843 °C (1625 °F)	926 °C (1700 °F)
Carbon potential	0.8 %C	0.6 %C	0.7 %C
Soak time	90 min	90 min	90 min
Atmosphere	Endothermic gas		
Quenching	Oil 60 °C (140 °F)		
Tempering	177 °C (350 °F) for 1 hour		

Testing
MPIF Standard Test Methods[3] were used for mechanical testing. Carbon and oxygen contents were determined using "Leco" infrared combustion analyzers according to ASTM E 1019-02. Dimensional change was tested on TRS bars after heat treatment according to MPIF standard 44. Apparent hardness, transverse rupture strength and impact energy were evaluated as heat treated for all densities and heat treatments per MPIF standards 43, 44 and 40. Determination of effective case depth for material A, were performed according to MPIF standard 52. Jominy hardenability test was performed according to ASTM standard A255-07.

Plane four point bending displacement control fatigue tests with load ratio R=-1, i.e. fully reversed loading at 25 – 30 Hz were performed using the staircase method. Tests were terminated after either 2.5% reduced stiffness or after the run out limit 2 million cycles was reached. MPIF standard 56 was used to evaluate the 50% probability limit $\sigma_{50\%}$ and standard deviation ω. The calculated value was accepted as fatigue limit provided that a clear plateau was displayed in the S-N curve at less than one million cycles. 90% probability limit $\sigma_{90\%}$ is calculated according to the same standard from $\sigma_{50\%}$, ω and number of test bars included in the staircase.

Metallography
Samples were rough cut from the desired areas of the tests specimens using a Struers Discotom-5 saw via 60A25 Cut-off blade. The specimens were mounted into cylindrical pucks ("Isofast" – for surface layer and Bakelite "Malifast" – as body). Depending on the specimen size, a LaboPress-3 (40 mm diameter mount) or Buehler Simplimet-2000 (25 mm diameter mount) mounting press was used.

The mounted specimens were secured into a sample holder and ground using Struers Abraplan for 10–15 seconds on Al_2O_3 stone to achieve a flat surface and eliminate possible distortions from the saw. After grinding, the specimens were washed with water. Fine grinding with MD-Allegro 9µm disk using DP-Suspension M-9µm was completed using a Struers RotoPol-22–RotoForce-4 automatic polishing machine with a Multidoser system. This automatic system was also used for the polishing steps.

After the 9µm grinding the samples were cleaned with alcohol in an ultrasonic apparatus for 3–4 minutes and dried with compressed air. The clean mounts were polished with MD-Mol 3µm disk using DP-Suspension M-3µm (5–7 drops/min) for 6–12 minutes to open the porosity. The samples were cleaned with alcohol and dried with compressed air. Final polishing was done with MD-Nap 1µm disk using DP-Suspension M-1µm for 25 seconds. Struers blue DP-Lubricant (4–7 drops/minute) was used during 9µm grinding and polishing processes.

The polished samples were observed using Leica optical microscope with x5–x50 magnification lenses. Unetched microstructures were captured using Olympus digital video camera system. The unetched samples were tested for microindentation hardness using a Buehler-8540HT microindentation hardness test machine.

As Astaloy CMN is a prealloyed material with low Cr-content, the Nital + Picral etchant was chosen to develop good contrast between pearlite-bainite and martensite and lower bainite. The etchant composition was 100ml 95% Ethyl alcohol + 4g Picric acid + 1ml HNO_3. Etching time of 3–20 sec. was used depending on the carbon content. The etched microstructures and microindentation hardness were investigated using same equipment.

RESULTS AND DISCUSSION

Density

Table V shows the densities obtained after heat-treatment of materials A and B.

Table V. Heat treated densities of materials A and B

	A_{CQT}		$B6_{QT}$		$B7_{QT}$	
Specimen	A^{7}	A^{73}	$B6^{71}$	$B6^{73}$	$B7^{7}$	$B7^{73}$
TRS	7.00	7.26	7.11	7.29	7.04	–
Ø25	–	–	–	–	7.00	7.30
Ø38	–	–	–	–	7.00	–
Jominy	–	–	–	–	6.90	–

Designations: A_{CQT} – Carburized-Quenched-Tempered material A; $B6_{QT}$ and $B7_{QT}$ – Quenched-Tempered materials B; A^{73} etc. – material at density (7.3 g/cm³)

Carbon and Oxygen

Carbon and oxygen contents after heat-treatment are shown in Table VI. The oxygen contents are typical for heat treated PM alloys.

Table VI. Carbon and Oxygen after heat-treatment

Materials	C, %	O_2, %
A^{7}_{CQT}	0.63	0.23
A^{72}_{CQT}	0.52	0.20
A^{73}_{CQT}	0.45	0.13
$B6^{71}_{QT}$	0.65	0.12
$B6^{73}_{QT}$	0.52	0.11

Dimensional Change

Dimensional change from die - sintered and die - heat treated was evaluated, see Figure 3.

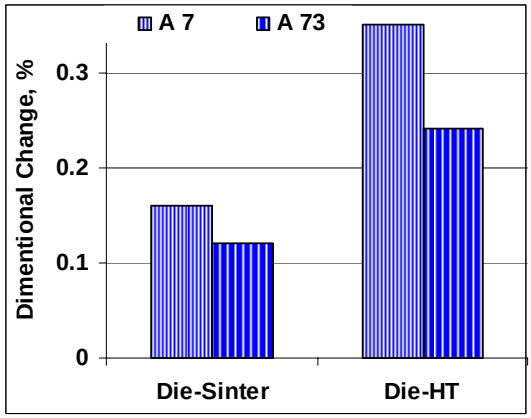

Figure 3. Dimensional change of material A.

Apparent Hardness
Figure 4 shows the apparent hardness of TRS bars (similar to other specimens) achieved after heat treatment.

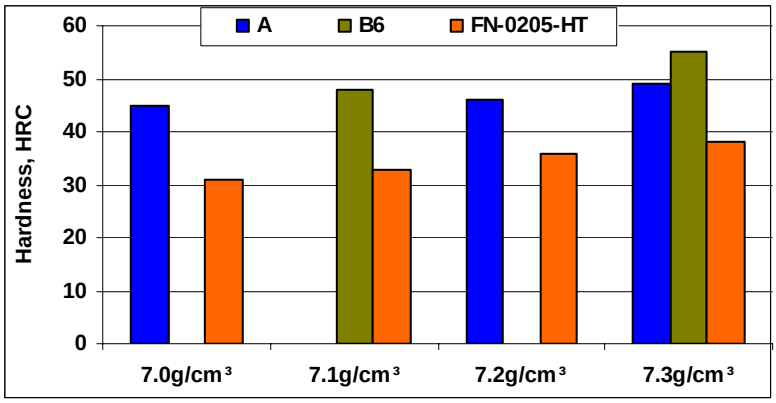

Figure 4. Hardness of Astaloy CMN in the heat treated condition compared to FN-0205-HT.

The materials show normal trends for apparent hardness increases with increased density and carbon content. After heat-treatment the apparent hardness appears much higher than FN-0205-HT (there is no standard for CQT). The high apparent hardness observed in all cases is due to the net effect of the combination of Cr and Ni in the base powder.

Microindentation hardness: Materials and Processes
Material A
The microindentation hardness profile of case carburized TRS bars and Ø25 cylinder from material A at different densities measured from the surface is reported in Figure 5.

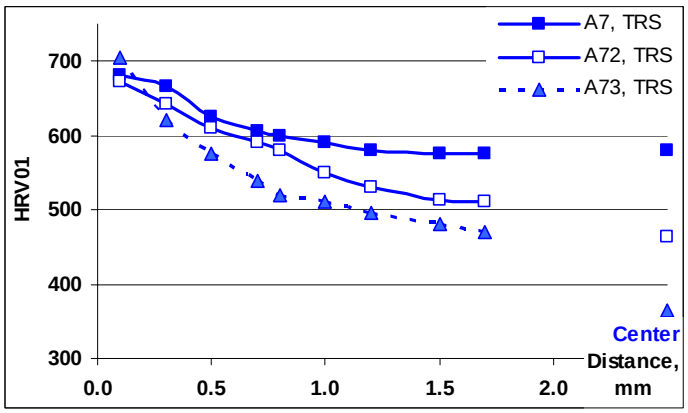

Figure 5. Microindentation hardness (100g load) of carburized material A.

The case depth depends on density. TRS bars at approximately 7.00 g/cm³ were through hardened while at 7.30 g/cm³ both specimens obtained a well defined case. The effective case depth at a minimum of 515 $HV_{0.1}$ (equivalent to ~50 HRC) obtained was 1.5 mm at a density 7.30 g/cm³ (Table IV).

Material B

The microindentation hardness of TRS bars (as an average of 3 bars and 5 readings on each specimen) after through hardening is shown in Figure 6 compared to standard data.

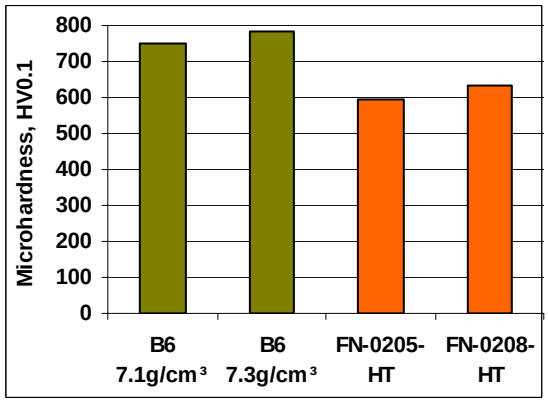

Figure 6. Microindentation hardness of material B.

Microindentation hardnesses up to 790 $HV_{0.1}$ were achieved, which is equivalent up to 64 HRC. This exceeds FN-0205-HT and FN-0208-HT requirements.

Microhardness: Mass Effect

The microindentation hardness profile of through hardened cylindrical specimens (Ø25x25 mm and Ø38x38) manufactured from material B7 at different densities is reported in Figure 7.

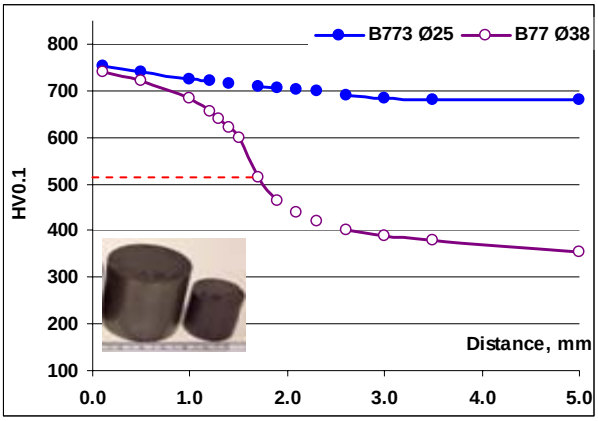

Figure 7. microindentation hardness of material B7 after through.

The smaller cylinder Ø25 mm was through hardened. When the mass/volume ratio of the specimens is increased, the core hardness reduces accordingly. The material shows good hardenability.

Transverse Rupture Strength
Figure 8 shows the transverse rupture strengths of heat treated materials at different densities compared to FN-0205-HT steel.

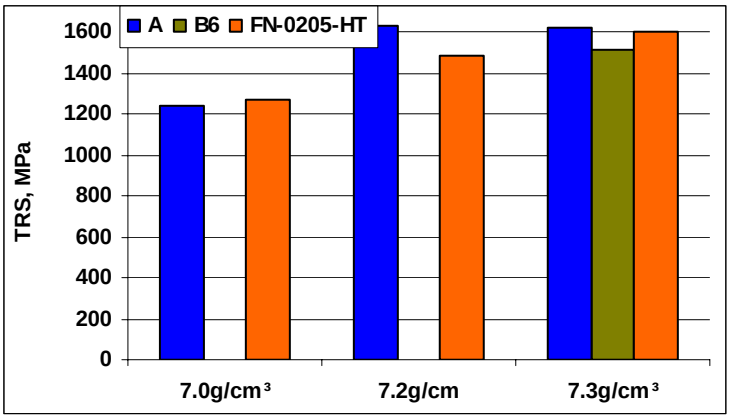

Figure 8. TRS at different densities compared to FN-0205-HT.

The result of this trial shows Astaloy CMN is comparable to FN-0205-HT standard data.

Impact Energy
Unnotched impact energy of material B6 after heat treatment is shown in Figure 9.

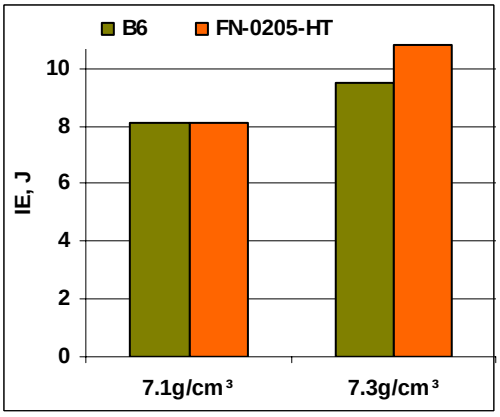

Figure 9. Impact Energy of material B6 compared to FN-0205-HT.

The impact energy increased with increases in density and was very similar to FN-0205-HT steel.

Fatigue Strength

The plane bending fatigue performance of the case carburized material A is shown in Figure 10 at 50 and 90% probability of survival. The error bars show the standard deviation of the measurement. The fatigue limit for the FN0208-HT is taken from the MPIF standard 35.

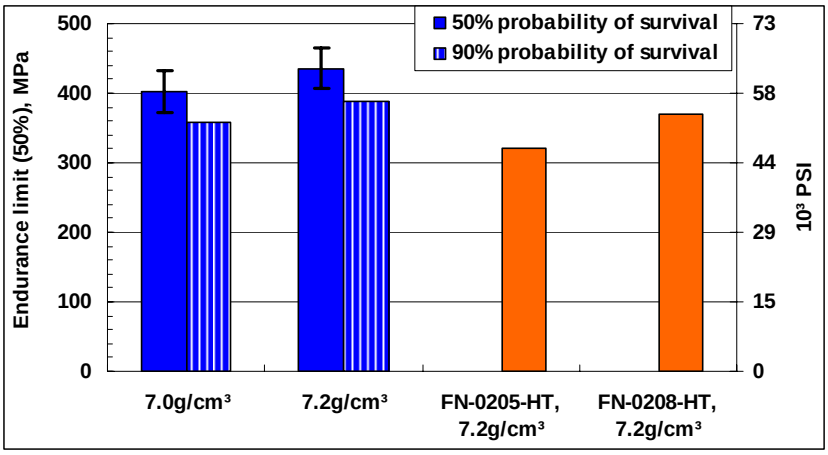

Figure 10. Fatigue limit of the case carburized material A at 50 and 90% probability of survival.

Table VII shows obtained data compared to FN-0208-HT at three densities from MPIF standard 35.

Table VII. Fatigue performance of the case hardened materials.

Material	Density, g/cm³	Fatigue limit 50% survival. MPa	Standard deviation, MPa	Fatigue limit 90% survival, MPa
A[7]	7.0	402	30	357
A[72]	7.2	436	30	388
FN-0205-HT	7.0	-	-	320
FN-0208-HT	7.2	-	-	370

Material A shows a higher performance than the FN-0208-HT material. Differences between materials and even between series of the same materials are normally due to processing, especially martensite gradients that create compressive residual stresses. Astaloy CMN produced a very uniform microstructure because it is prealloyed. The FN-02XX-HT materials will have Ni-reach austenite areas, which will be much softer than the majority martensitic structure. This difference impressed fatigue. Residual stresses were not determined in this investigation. The important conclusion is material A has shown to respond well to the case carburizing process.

The fatigue data generated by the rotating beam method can be directly compared to four point plane bending data under certain conditions. On the rotating beam specimens the crack initiates on the surface of the specimen. Systematic errors can be introduced by the required machining of the surface, both increasing and decreasing the fatigue performance of the specimens. However, such problems will not be discussed in this context. The four point bending fatigue test specimens have two surfaces that reach the maximum stress. A careful analysis shows that the transition from plane stress at the surface to plane strain in the core results in stress maxima at the corners and at the middle of these surfaces[4]. The crack initiation at the corners is suppressed by mild grinding of the edges in order to smooth the surface and remove the burr from the compaction. If the crack initiation at the middle of the surfaces is dominating the failures the fatigue limit will be very close to what is measured by the rotating beam method.

Jominy Hardenability test

Jominy hardenability tests for material B were performed by Modern Industries, Inc. according to ASTM standard A255-07. The machined specimen was austenized at 926°C (1700°F) prior to performing the Jominy end quench. Figure 11 shows a Jominy hardenability test bar sectioned for metallography and microindentation hardness measurements compared to FN-0205-HT steel.

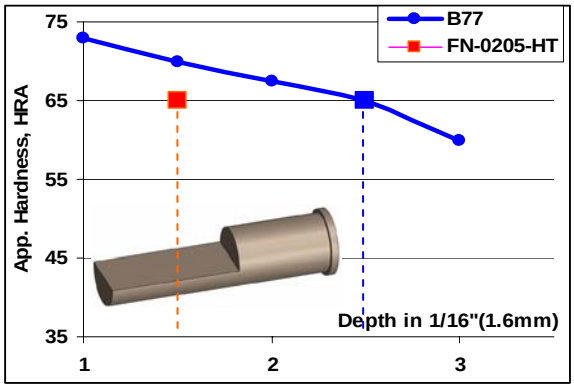

Figure 11. Jominy hardenability tests compared to FN-0205-HT.

Material B reached the required hardness of 65HRa in depth of 2.5 J-steps (4.0 mm) compared to 1.5 J-steps (2.4 mm) for FN-0205-HT steel, which indicated that Astaloy CMN exhibits better hardenability then FN-0205-HT steel.

Microstructures

A typical unetched microstructure obtained after heat treatment is shown in Figure 12 (left). The oxygen contents shown in Table VI are not present as grain boundary oxides in the microstructure. Figure 12 (right) shows a typical etched microstructure at the surface.. The surface microstructure was similar for both materials and heat treatments. For both materials a martensitic microstructure was developed. Due to high carbon content at the surface plate martensite was generated.

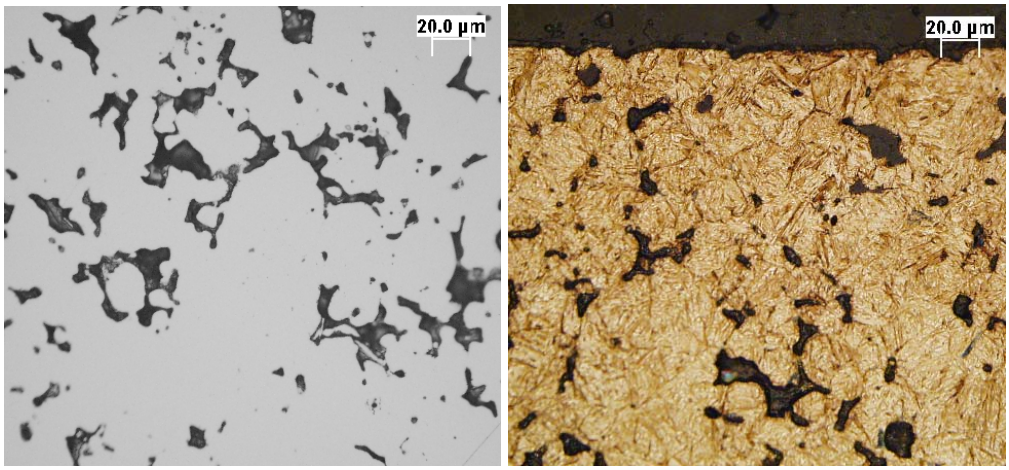

Figure 12. Typical unetched and etched microstructures of materials A (surface) and B.

Material B

The mass effect study microstructures are presented in Figure 13a–b (see Figure 6 microindentation hardness section above). The microstructure the in center of the Ø25 mm cylinder (Figure 13a) contained lath martensite (low carbon) and dense pearlite mixed with some dense bainite. The center area of the Ø38 mm cylinder (Figure 14b) had lath martensite and more dense pearlite. A small amount of dense bainite as well as ferrite in the grain boundaries also could be found.

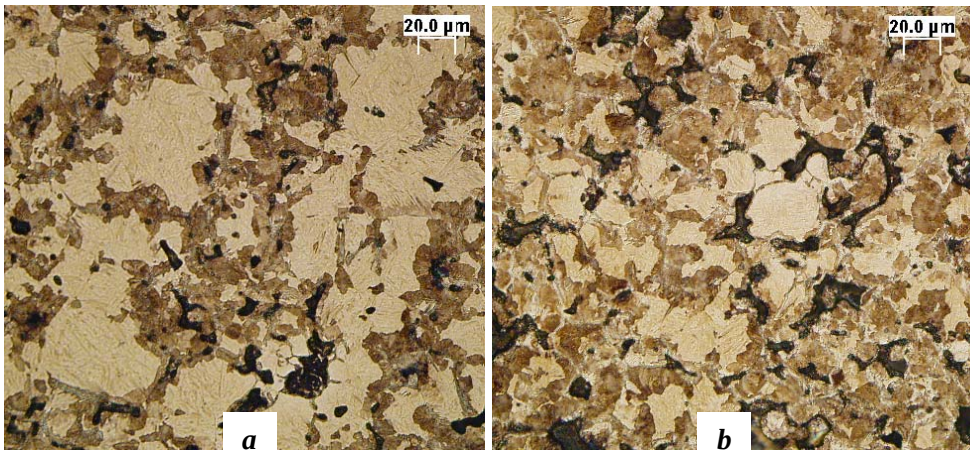

Figure 13. Material B7 microstructures in center areas: *a* – cylinder Ø25mm; *b* – Ø38mm.

All microstructures show good correlations with test data and microindentation hardness profiles described above.

CASE STUDY

Gas carburization of spur gears

Usually gears require a hard surface and a tough core. These features are commonly achieved by case hardening operations. Based on the results obtained with the test specimens, the case-carburization of FZG gear manufactured from material A was performed. The gear, shown in Figure 14, had a diameter Ø82.26 mm (Ø3.24”), height 15 mm (0.59”) and 16 teeth. The gears were compacted to a green density of 7.2 g/cm^3. Sintering was carried out using the same equipment and conditions as described in Table III. The carburization was carried out at Pennsylvania Industrial Heat Treaters in the same equipment used for the test bars with different austenization condition.

An apparent hardness of 47 HRC was achieved in the surface of the heat treated gears. The microindentation hardness obtained in the case and the core of a gear tooth is shown in Figure 14.

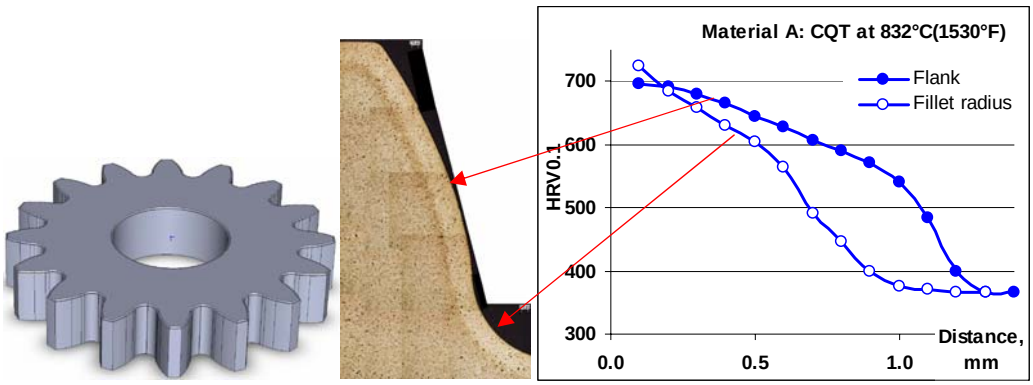

Figure 14. Microindentation hardness of case carburized spur gear.

A microindentation hardness of up to 740 $HV_{0.1}$ was achieved in the surface. A case depth of 515 $HV_{0.1}$ (equal to 50 HRC) is required for gears. The microindentation hardness profile measured perpendicular from the surface and inwards showed a case depth of 0.6mm (fillet radius) and 1.1mm (flank). The microstructure in the case is martensite similar to Figure 12 shown above. In the core, a softer microstructure predominantly dense pearlite/upper bainite and ferrite in the grain boundaries was formed.

The result obtained with case carburization on the gears corresponds with the results obtained from the test bars regarding both the microstructure and microindentation hardness profile. The data generated for test bars can therefore be used in the design of components similar to gears. Depending on the component geometry and size the parameters used for carburization should be optimized to obtain the required case depth and microhardness profile.

CONCLUSIONS

- Astaloy CMN, a lean Cr-Ni alloy, suitable for different types of heat treatments.
- A hardness level up to 50 HRC could be obtained after heat treatment. The hardenability of the alloy is superior to FN-020X-HT PM steel.
- Astaloy CMN achieves high Fatigue limit (90% probability of survival) of 357 and 388 MPa at densities of 7.0 and 7.2 g/cc respectively. These fatigue limits are higher than FN-020X-HT due to uniform microstructure achieved.
- The combined hardness, uniform microstructure and fatigue properties make Astaloy CMN suitable for conversion of heat treated wrought materials to PM.

References

1. Nagarjuna Nandivada, David Milligan, Alexander Klekovkin, Yoshinobu Takeda and Yang Yu, "Performance Characteristics of a Newly Developed Cost-Effective Cr-Ni Prealloyed Steel Designed to replace Fe-Ni Steels", *Advances in Powder Metallurgy & Particular Materials*, compiled by Roger Lawcock, Alan Lawley, FAPMI, Patrick J. McGeehan, Metal Powder Industries Federation, Princeton, NJ, 2008, part 7, pp. 7-85 – 7-97.
2. *MPIF Standard 35 Materials Standards for PM Structural Parts*, 2007, Metal Powder Industries Federation, Princeton, NJ.
3. *MPIF Standard Test Methods*, 2008, Metal Powder Industries Federation, Princeton, NJ.
4. A. Bergmark, S. Bengtsson, Fatigue properties of Cu-C alloyed PM steels at two density levels, Euro PM 2001, European Congress and Exhibition on Powder Metallurgy, Nice, France, October 22-24, Vol. 2, 110-115.